Journal of Information Systems Engineering and Management
2025, 10(7s)
e-ISSN: 2468-4376
https://www.jisem-journal.com/

Research Article

Assessment of Return Periods for Flood Frequency and Risk Mapping of Floods and Cyclones in India using Arcgis

*Rajani Kant Awasthi, Dr. Atul Sangal
Sharda University, Greater Noida, Uttar Pradesh, India
rka0285058@gmail.com

ARTICLE INFO

Received: 04 Oct 2024

Revised: 12 Dec 2024

Accepted: 20 Dec 2024

ABSTRACT

Due to its diverse geography and climate, India is highly susceptible to natural disasters like floods and cyclones, with an 8,000-kilometer coastline exposed to 10% of the world's tropical storms, five to six form annually, with the Bay of Bengal being particularly affected due to its higher frequency. This study aims to conduct a detailed flood frequency analysis and risk mapping for the 2014 Srinagar flood, utilizing statistical techniques and GIS-based tools to evaluate the return periods and recurrence frequencies. The study incorporates data from three gauging stations, Asham, Sangam, and Ram Munsi Bagh, regarding discharge rates in cubic meters per second (cms). Statistical models were applied, including Normal, Log-Normal, Log-Pearson Type III, and Gumbel distributions. GIS data was sourced from USGS, DIVA-GIS, and WorldClim to assess flood risk and affected areas. The study's result revealed that while Log-Normal and Log-Pearson models did not exceed threshold values, the Gumbel distribution indicated potential exceedance at a 95% confidence level, suggesting enhanced safety measures were needed. The analysis shows varying risk levels across gauging stations, with recommendations for improved flood management strategies, especially for areas prone to high flood risk. Further research should focus on refining flood prediction models, enhancing GIS capabilities for risk assessment, and implementing comprehensive flood mitigation strategies.

Keywords: Return Period, Frequency, Discharge Flow, Distribution Curve, Exceedance Probability, ArcGIS, Arc Scene, 3D Modell.

INTRODUCTION

With its diverse geography and climate, India is highly susceptible to natural disasters like floods and cyclones. The country's coastline is exposed to 10% of the world's tropical storms, with five to six forming annually. The Bay of Bengal is known for its higher frequency of cyclones (Sahoo & Bhaskaran, 2016). It is believed that about 40 million hectares, or 12% of India's geographical area, iss vulnerable to flood risks (Deshpande, 2022). Urban areas are increasingly vulnerable due to inadequate drainage systems and rapid urbanization, leading to economic losses and population displacement.

In September 2014, massive floods in Jammu and Kashmir were observed, caused by heavy and continuous rainfall that lasted for a week (Mishra, 2015). Many of the Anantnag, Pulwama, Baramulla, Bandipora, and Srinagar districts were submerged (Bhat et al., 2019). The severity of the flood was quite massive, and the preparedness to face such a catastrophic event at the local level was also resilient; therefore, possible help and necessary support could be possible by the agencies responsible after passing significant period. All the services were at halt due to severity of the flood and huge economic loss was envisaged in terms of direct losses to the tune of approximately 20 billion dollars and indirect losses of around 16.74 billion dollars.

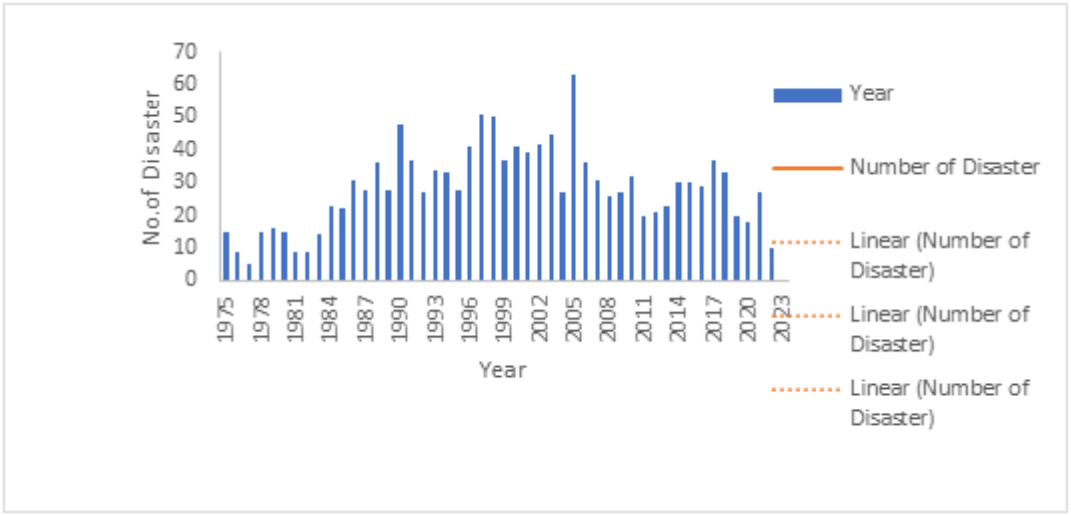

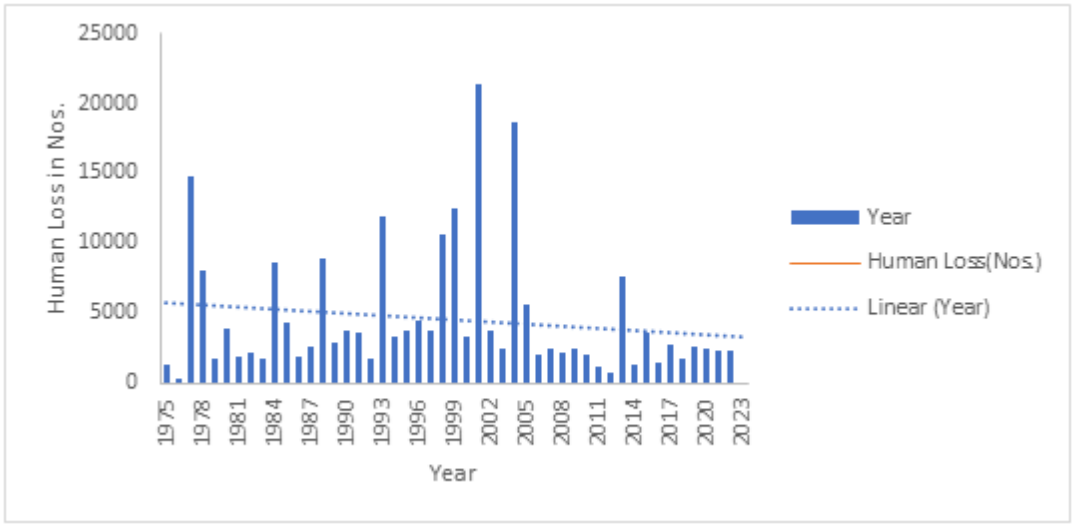

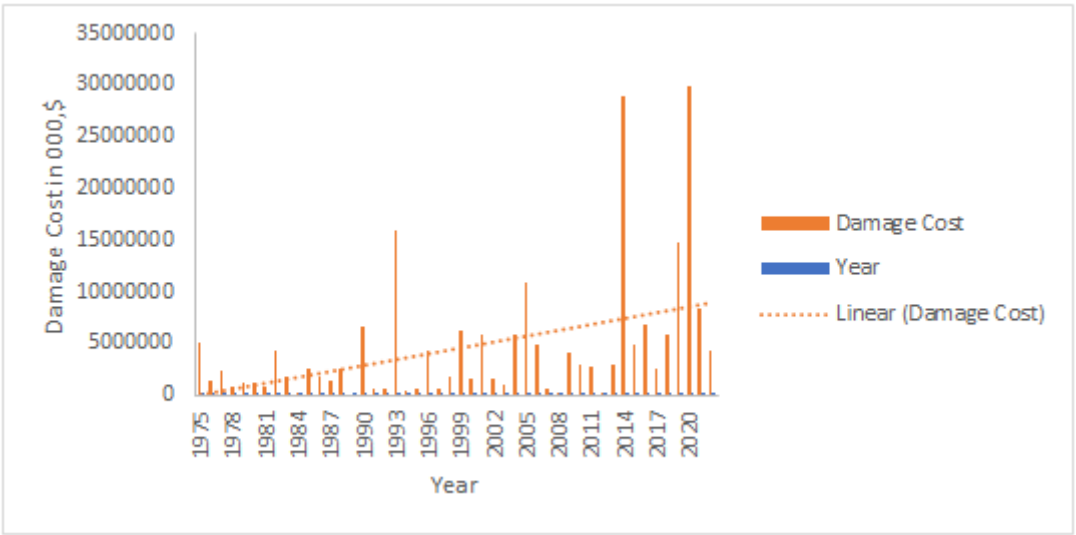

Figure 1: A glimpse over the history of Natural disasters in India

Figure 1 shows a decreasing trend in human losses but an increasing trend in damage cost due to India's developing status. The top graph shows a growing trend in natural disasters, with spikes in certain years indicating potential clusters of severe weather events. The bottom graph shows the financial damages caused by these disasters, with an upward trend indicating an escalating economic impact. The image aligns with the research's aim to analyze India's

frequency and effects of natural disasters, particularly floods, to identify patterns, examine correlations between disaster numbers, human loss, and damage cost, and assess future risks for preparedness and mitigation strategies.

Flood frequency analysis is crucial in India, where 40% of natural disasters involve floods and cyclones. The 2014 Kashmir flood was a major event, causing significant loss of infrastructure and human lives with a peak discharge of 1699 cus at Asham, 3398 cus at Sangam, and 1982 cus at Ram Munsi Bagh gauging station (Malik, 2022; Mishra, 2015). Water resources design and management require analyzing extreme flood events, particularly those with defined return periods. The annual block maxima approach is a common method used, where peak streamflow is determined each year, and a distribution fitted to it is used to estimate the return level for a defined period (Langat et al., 2019). This approach is essential for managing water resources effectively and minimizing the impact of floods.

In many case studies, the implementation of historical data into flood frequency analysis was demonstrated, e.g., by using traditional methods of statistical analysis (Frances et al., 1994; Kjeldsen et al., 2014; Sartor et al., 2010) or Bayesian statistics (Gaál et al., 2015; Payrastre et al., 2011; Viglione et al., 2013), Frances et al. (1994) conducted a systematic study which assesses the effectiveness of incorporating historical flood data in flood frequency analysis, comparing its impact with systematic records, examining factors like record length, flood return periods, and threshold levels (Frances et al., 1994).

Strupczewski et al. (2014) examined the impact of the largest historical flood on flood frequency analysis in Srinagar, the most affected region in Jammu and Kashmir province. The authors have used the Weibull and Gumbel distribution to analyze the flooding extent in various neighborhoods, including Sonwar Bagh, Shivpora, Batwara, Soitang, Lasjan, Padshai Bagh, Natipora, Lal Chowk, Rajbagh, Jawahar Nagar, and Wazir Bagh (Strupczewski et al., 2014).

However, the current study aims to enhance India's disaster management and mitigation strategies using ArcGIS tools. The study aims to improve preparedness and response planning for flood disasters by understanding return periods and risk mapping. Floods and cyclones are two of India's most recurrent and devastating natural hazards. The study uses ArcGIS to determine the return period for flood frequency and create risk maps. The return period estimates the likelihood of a flood event occurring within a given period, helping design infrastructure that can withstand extreme events and inform policy decisions. The risk mapping integrates historical flood records, topography, land use, and population density, identifying high-risk areas and developing targeted risk reduction strategies.

DATA AND METHODS

2.1 Data Collection

2.1.1 Gauging Stations

- **Locations:** The data for the current study was collected from three gauging stations in India: Asham, Sangam, and Ram Munshi Bagh
- **Discharge Rates:** The discharge rate in cubic meters per second (cms) at these gauging stations was obtained from the state government's website.

2.1.2 GIS Data

- **Sources:** GIS data for the study have been taken from USGS, DIVA-GIS and WorldClim.

2.2 Flood Modeling Methods

In the present study, the following methods have been employed for flood modeling:

2.2.1 Normal Distribution

The normal distribution is very typical in the technical analysis of the stock market and has mean and standard deviation parameters (Sahu & Sahu, 2016). Like any other data set, it consists of an average, median, and mode; the apex denotes the highest point. This distribution is vital in deriving the Central Limit Theorem (CLT), whereby averages from independent identically distributed random variables are approximated by normal distribution (Bera et al., 2016).

However, as can be observed, only the mean (μ) and the standard deviation (σ) are required for the computation.

$$F(x) = \frac{1}{\sigma\sqrt{2\pi}}\, e^{-\frac{1}{2}(\frac{x-\mu}{\sigma})^2}$$

Where,

x = value of the variable or data being examined and f(x) the probability function

μ = the mean

σ = the standard deviation

- **T-Year Flood Estimation:**

T-year flood estimates can be graphically or analytically, with the main drawback being that different individuals may receive different forecast. Analytical methods use parameter estimation using the Method of Moment.

In normal distribution, T-year flood is given by:

$$X_t = \overline{x} + K_T S_x$$

Where,

x^- = Sample mean

S_X = Sample Standard Deviation

K_T = Frequency factor corresponding to probability of exceedance

2.2.2 Log-Normal Distribution:

This distribution is utilized when the data's logarithms match a normal distribution.

(Crow & Shimizu, 1987)

Probability Distribution Function: $F(x) = \frac{1}{x\sigma_y\sqrt{2\pi}} e^{-\frac{[logx-\mu y]^2}{2\sigma 2y}}$

- **T-Year Flood Estimation:**

$$X_{T=}\, e^{\overline{z}+K_T\sigma_z}$$

2.2.3 Log-Pearson Type III Distribution:

This distribution is often utilized in the USA for government-sponsored projects (Kumar et al., 2020). After converting the data into base ten logarithmic form, analysis shows that the series of Z also varies if X is the variate of a random hydrologic series.

Hence,

Z = log X

$$X_T = 10^{Zr}$$

$$Z_T = \overline{z} + Kz\sigma_z$$

K_Z = a frequency factor which is a function of recurrence interval T and the coefficient of skew Cs,

σz = Standard deviation of the Z variate sample

2.2.4 Gumbel Distribution:

Gumbel introduces the Gumbel model, an extension of the exponential distribution, which offers an increasing or decreasing hazard function, unlike the constant exponential distribution (Fayomi et al., 2022). Gumbel's model is a widely used distribution for fitting extreme data sets in various scientific fields, including hydrology, meteorology, climatology, insurance, finance, and geology, as demonstrated in a study by Gumez et al. (2019) (Gómez et al.,

2019). In hydrologic and meteorological research, it is one of the most often used probability distribution functions for extreme values, used to estimate flood peaks, maximum rainfall, maximum wind, etc.

- **Probability Formula:**

$$P(X \geq x_0) = 1 - e^{-e^{-y}}$$

Where y is a dimensionless variable given by:

- **T-Year Flood Estimation:**

$$X_T = \overline{x} + K\sigma_z$$

$$y_T = -In[In\left(\frac{T}{T-1}\right)]$$

$$K = \frac{(yr - 0.577)}{1.2825}$$

2.3 Goodness-of-Fit Tests

2.3.1 Chi-Square Test:

The chi-square test for goodness of fit involves comparing frequencies of a variable with expected values derived from the assumed theoretical distribution model (Collins et al., 1993). The test is based on the quantity distribution, which asymptotically approaches the chi-square distribution with a k-1 degree of freedom. Suppose the parameters of the theoretical model are unspecified and have to be determined from the data at hand. In that case, the degrees of freedom will have to be decremented by one for every unspecified parameter to be estimated.

Suppose the assumed distribution gives the value of ∑i=1K (ni − ei)2 /ei < C1-α. f, the assumed theoretical distribution is an acceptable model; otherwise, the assumed distribution model does not support the observed data at the α significance level. For satisfactory results, it is generally necessary to have k>=5 and ei>=5. A chi-square (X2) goodness of fit test has been conducted for a categorical variable, assessing how well a statistical model fits a set of observations.

- **Test Statistics:**

$$X^2 = \sum \frac{k}{i=i} \frac{(ni - ei)^2}{ei}$$

H_o: The population does follow the specified distribution.

H_a : The population does not follow the specified distribution.

2.3.2 Kolmogorov-Smirnov (K-S) Test:

The K-S test measures the difference between the cumulative frequency from experiments with the cumulative distribution of an assumed theoretical distribution (Cox et al., 1988). This means that if the observed difference is greater than anticipated for the particular number of subjects in the sample, then the theoretical distribution cannot be used to model the given population. If the statistical value of the difference is less than the critical value, the theoretical distribution is acceptable at a specified level of significance.

$$D_n = \max | F_x(x) - S_n(x)|$$

The K-S test determines a random variable's maximum difference, Dn, with the critical value, Dn α, at a particular significance level α. The proposed theoretical distribution is acceptable if Dn is less than the critical value. The K-S test has an advantage over the chi-square test, which doesn't require data division into intervals (Kim & Whitt, 2015).

2.3.3 The Anderson Darling (A-D) Test:

The Anderson-Darling (A-D) Test, introduced by Anderson and Darling in 1954, is a statistical method that emphasizes the importance of the tails of a distribution (Aboraya et al., 2022; Raschke, 2020). It is valid for sample sizes larger than 7, as it is expressed in logarithms of probabilities. The critical value (cα) and adjusted A-D statistic

(A*) are based on the form of the proposed theoretical distribution and sample size (n), as defined in the table under the appendix.

- **Test Statistics:**

$$A^2 = -n - \frac{1}{n}\sum \frac{n}{i=i}(2i-i)[In\ Fx(xi) + In(1 - Fx(x_{n+1-i}))]$$

- **Adjusted Statistics:**

$$A^* = A^2(1 + \frac{0.2}{\sqrt{n}})$$

RESULTS AND DISCUSSIONS

3.1 Performance Indicators

Table 1 presents the performance indicators for the Ram Munsi Bagh gauging station, comparing Normal, Log-Normal, and Log-Pearson Type III distributions. The Normal distribution shows high accuracy with an R^2 of 0.98 and IA of 0.9999 but a higher RMSE (1.036) and MAE (75.76). The Log-Normal distribution has lower accuracy (R^2 = 0.75, IA = 0.9366) but reduced MAE (0.485). The Log-Pearson Type III distribution simplifies to Log-Normal due to zero skewness (Cs = 0).

Table 1: Performance Indicator for Ram Munsi Bagh gauging station

Distribution		NAE	RMSE	MAE	PA	R^2	IA
Normal	μ=756.87 σ=404.58	1.036	75.76	0.574	0	0.98	0.9999
Log-Normal	μ=0.7243 σ=0.032	1.181	0.485	0.248	0	0.75	0.9366
Log-Pearson Type-III	Cs=0, hence log -Pearson Type III reduces to Log normal distribution Cs(Coefficient of skewness)=N∑(Z-Zbar)^3/(N-1)(N-2)σz^3						

Normalized Absolute Error = $\sum^{N}_{i=1}$(Ypred. -Yreal)/$\sum^{N}_{i=1}$Yreal

Root Mean Square Error = $\sqrt{(Y\hat{}_i - Yi)^2/n}$

Mean Absolute Error = $\sum^{n}_{i=1}(y_i - x_i)/n$

Prediction Accuracy = $\sum^{n}_{i=1}(Yi- Y\hat{})(Xi-X\hat{})/(n-1)\sigma_P\ \sigma_{o[}$

R^2(Coeff. Of Determination) = $[\sum^{n}_{i=1}(Yi- Y\hat{})(Xi-Xi\hat{})/nS_PS_o]^2$

Index of Accuracy = $1-\sum^{n}_{i=1}(Y\hat{}_i - Yi)^2/\sum^{n}_{i=1}[(Yi- X\hat{})+(Xi- Xi\hat{})]^2$

n = no. of observations, Yi=Predicted value, Oi=Observed value, $Y\hat{}_i$=Mean of predicted value

$Xi\hat{}$=Mean of observed value, Sp=S.D. of predicted value, So=S.D. of the observed value

3.2 Flood Frequency

Table 2 highlights the flood frequency estimates for the Jhelum River at Ram Munsi Bagh gauging station. The highest discharge estimate is 1895.11 cms for a 50-year return period using the Log-Normal distribution, while the lowest is 1055.71 cms for a 5-year return period using the Gumbel distribution. These figures reflect the variability in discharge predictions depending on the statistical distribution model and return period used.

Table 2: Flood Frequency estimates of Jhelum River for Ram Munsi Bagh gauging station

Return Period (Years)	Pi (Exceedance Probability)	Qi(Non-Exceedance Probability)	w	KT	Annual Discharge cms-Normal Distribution	μ+σ* KT	Annual Discharge cmsLog Normal Distribution(LN2)	Annual Discharge cms Gumbel Distribution
5	0.2	0.80	1.7941	0.8414	1097.31	7.0108	1108.62	1055.71
10	0.1	0.90	2.1459	1.2817	1275.44	7.2055	1346.84	1296.68
15	0.06	0.93	2.3272	1.5013	1364.31	7.3026	1484.20	1432.63
20	0.05	0.95	2.4477	1.6452	1422.50	7.3662	1581.64	1527.82
25	0.04	0.96	2.5372	1.7510	1465.33	7.4130	1657.43	1601.15
30	0.03	0.96	2.6081	1.8343	1499.01	7.4498	1719.57	1660.80
35	0.02	0.97	2.6665	1.9026	1526.65	7.4800	1772.30	1711.08
40	0.02	0.97	2.7162	1.9603	1550.01	7.5051	1818.14	1754.54
45	0.02	0.97	2.7592	2.010	1570.21	7.5276	1858.71	1792.82
50	0.02	0.98	2.7971	2.0541	1587.96	7.5470	1895.11	1827.01

Pi=Exceedance Probability, qi=Non-Exceedance Probability

$W=(-2\text{Log}(P))^{1/2}$, P=1-F and $F=1-T^{-1}$

$K_T = W-(C_0+C_1W+C_2W^2) / (1+d_1W+d_2W^2+d_3W^3)+\varepsilon(P)$

$C_0=2.5155$, $C_1=0.8028$, $C_2=0.0103$, $d_1=1.4327$, $d_2=0.1892$, $d_3=0.0013$

Table 3 presents the Chi-Square Test results comparing observed flood frequencies with theoretical frequencies using Normal and Log-Normal distributions over different periods. The sum of the Chi-Square values for the Normal distribution is significantly higher (153.77) than the Log-Normal distribution (52.62), indicating a larger discrepancy between observed and expected frequencies for the Normal distribution. This suggests that the Log-Normal distribution may better fit the observed flood data at the Ram Munsi Bagh gauging station.

Table 3: Chi-Square Test

Year	Flood Frequency	Theoretical Frequencies		∑(ni – ei)²/ei	
		Normal	Log Normal	Normal	Log Normal
1979-82	12	22.96	8.80	5.231777003	4.531864093
1983-86	17	24.72	9.10	2.410938511	4.315671977
1987-90	13	32.27	8.80	11.50706229	4.417710968
1991-94	19	37.44	9.30	9.082094017	4.343350096
1995-98	18	42.85	9.30	14.41126021	4.417562817
1999-02	23	48.00	9.60	13.02083333	4.353107816
2003-06	46	46.17	10.50	0.000625948	4.238764344
2007-10	46	59.10	10.50	2.903722504	4.238764344
2011-14	25	64.43	9.60	24.1304501	4.241536014
2015-18	36	69.85	10.20	16.40404438	4.291943298
2019-22	17	74.54	9.00	44.41711296	4.225473073
∑				153.7705763	52.62475788

The critical Chi-square value of 113.14 indicates that the Chi-square test is valid for Log-normal tests only, allowing for modeling based on log normal distribution.

3.3 Log Pearson Type III Distribution

σZ=√((Σ(Sq(Z-Z(bar))/(N-1) = 0.334025046

Cs=N∑(Z-Zbar) ^3/(N-1) (N-2) σz^3

Cs=0, hence log -Pearson Type III distribution reduces to log normal, therefore detailed calculation for L of Pearson Type III.

Log Pearson Type III has not been carried out.

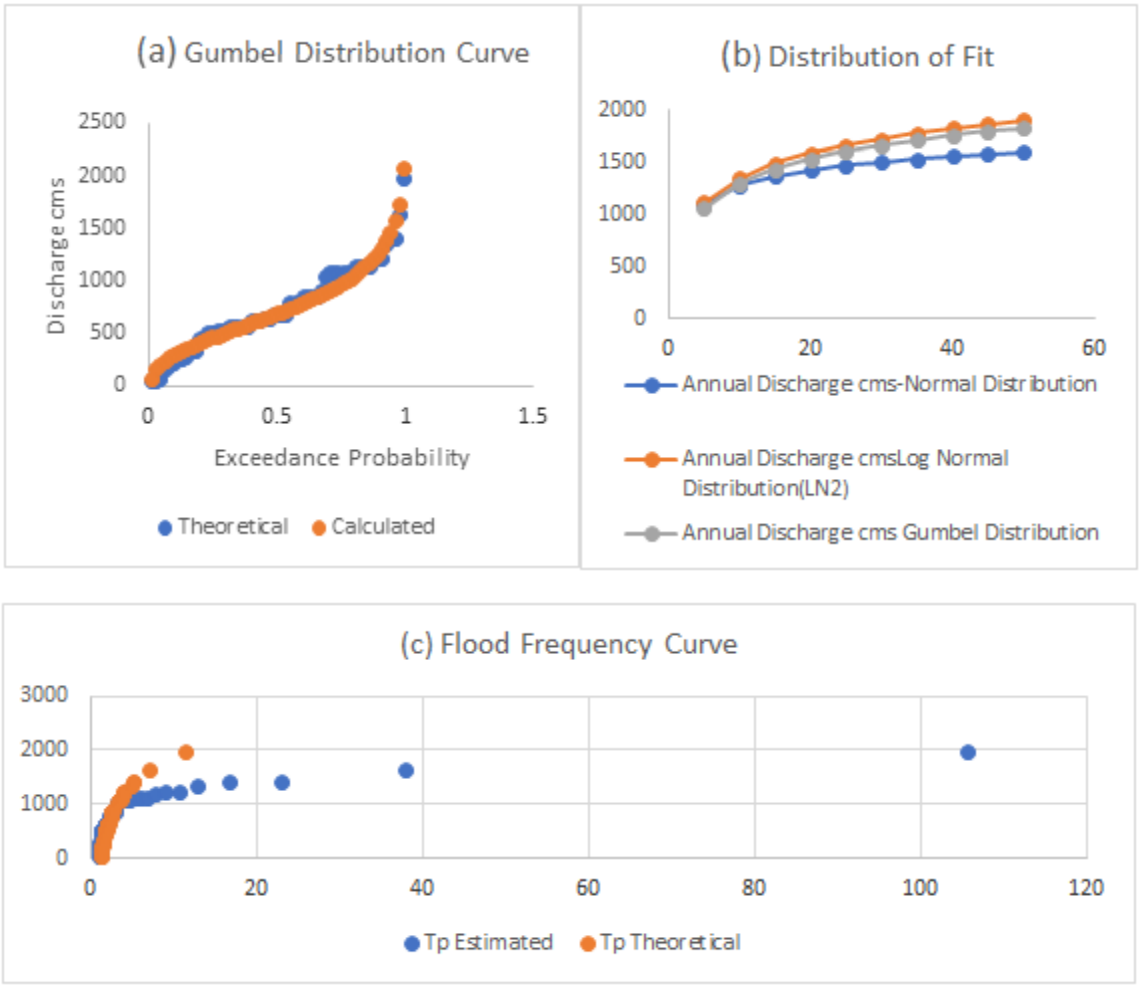

Figure 2: Comparison of Gumbel distribution fit, model fit, and flood frequency curve with peak discharge and return period

The graph consists of three components: The Gumbel Distribution Curve, which compares theoretical and calculated discharge values based on exceedance probability; the Distribution of Fit, plotting annual discharge against different models; and the Flood Frequency Curve, relating peak annual discharge to return period. The Gumbel distribution appears to be a reasonable fit for discharge data, showing an increasing trend with increasing return periods. However, further statistical analysis is needed to confirm this and assess the accuracy of the flood frequency curve.

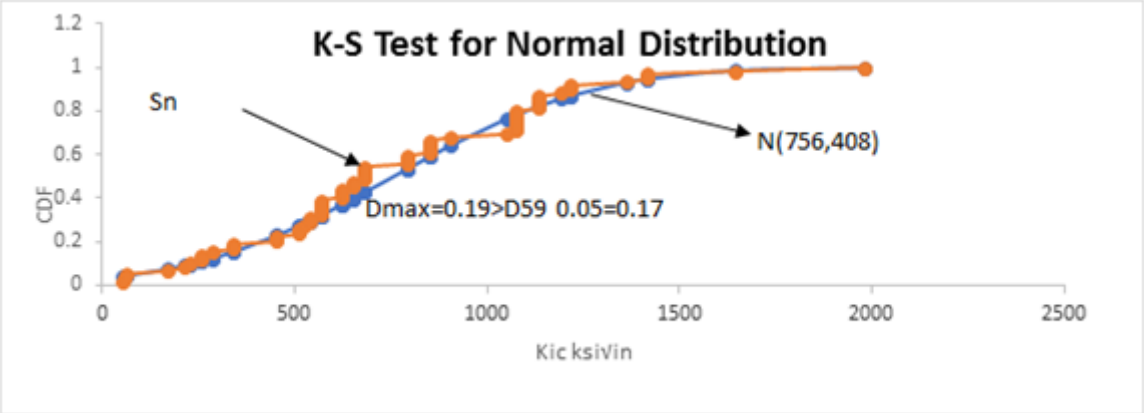

(a)

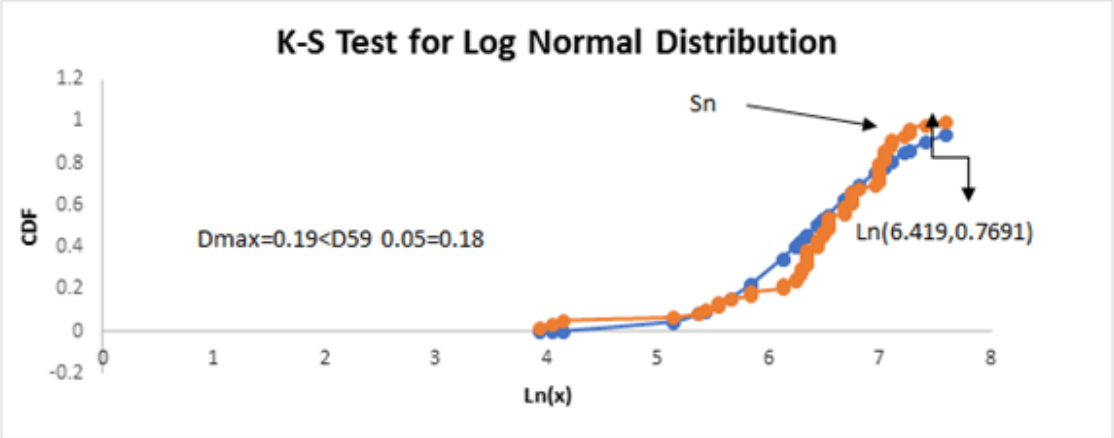

(b)

Figure 3: K-S Test

Figure 2 displays two graphs utilizing Kolmogorov-Smirnov (K-S) tests to evaluate data fit to distribution models. In Graph (a), the Normal Distribution's K-S statistic (Dmax = 0.19) exceeds the critical value (0.17), indicating a significant deviation from normality. In Graph (b), the Log-Normal Distribution's K-S statistic (Dmax = 0.19) is slightly below the critical value (0.18), suggesting a closer fit. However, the difference is minimal. While the data deviates from a normal distribution, further analysis is needed to confirm the log-normal fit.

K-S Test also qualifies to Log Normal Distribution as Dmax < Dn^{α}.

3.4 A-D Test for Gumbel Distribution:

Table 4 shows the Anderson-Darling (A-D) test results for the Gumbel distribution, which demonstrates an A-D statistic (A^2) of 0.0185 and an adjusted statistic (A*) of 0.0189. These values are significantly lower than the critical value (Cα) of 0.757, showing that the Gumbel distribution is compatible with the data. The low A-D statistic suggests a minimal deviation from the expected distribution, supporting the hypothesis that the data follows a Gumbel distribution.

Table 4: A-D Test for Gumbel Distribution

A^2(A-D Statistic.)	Adjusted. Statistic(A*)	Cα
0.018463967	0.01894473	0.757

As Adjusted. Statistic(A*) value (0.01894473) <Critical Value Cα (0.757)

Table 3 and Graph 3 (a) and (b) indicate that only Log Normal distribution has a qualified chi-square test, and Table 4 shows that the A-D test has a qualified Gumbel Distribution. Also Graph 2(a) shows a very good fit of

distribution for Gumbel distribution. However, it is evident from Table 2 that the calculated peak discharge in 50 years from any distribution cannot supersede the peak discharge of 1982 cms reached in the year 2014. Further, the study considered the goodness of fit by Gumbel distribution and calculated the upper and lower bound peak discharge at a 95 % confidence level.

									U_l	L_l
N	y_n	Sn	T_{50}	Y_{50}	K_{50}	x_{50}	b	Se	x_1	x_2
59	0.5527	1.177	50	3.901938658	2.845572	1908.149	3.688666	211.0537	2321.813694	1494.483

Value of Yn and Sn taken from Gumbel distribution table

Y_{50}=-Ln(Ln(T/T-1))

K_{50}= (Y_{50} –Yn)/Sn

$X_{50}=\mu + K_{50}*\sigma$

$b = \sqrt{(1+1.3* K_{50}+1.1* K_{50}^2)}$

$Se = b*\sigma/\sqrt{50}$

$Ui = X_{50} + 1.96*Se$

$Li = X_{50} – 1.96*Se$

The upper peak discharge flow, with a 95% confidence level, crosses the 1982 cum peak during the 2014 flood condition. This suggests a 95% (α = 0.05) probability of reoccurrence. The orange line in Graph 2(b) shows the theoretical distribution, while the blue line represents the fit of annual peak streamflow data with a Gumbel distribution, allowing for predictions of streamflow values for return periods ranging from 1 to 100 years. The study uses a Gumbel distribution curve to predict streamflow values for return periods from 1 to 100 years. However, the curve follows the distribution for low flows but drifts away from the theoretical distribution at higher flows. Therefore, multiple distributions are recommended, as this study follows this approach.

Table 5 presents performance indicators for the Sangam gauging station, comparing Normal, Log-Normal, and Log-Pearson Type III distributions. The Log-Normal distribution shows superior performance, with very low errors (NAE: 0.0002, RMSE: 0.475, MAE: 0.174) and a high index of agreement (IA: 0.9999), suggesting excellent predictive accuracy. The Normal distribution, while having a strong R^2 (0.92), has higher errors and a low percentage accuracy (0.00119). Overall, the Log-Normal distribution provides the best fit for the observed data.

Table 5: Performance Indicator for Sangam gauging station

Distribution		**NAE**	**RMSE**	**MAE**	**PA**	**R^2**	**IA**
Normal	μ=751.83	1.056	191.55	1.55	0.00119	0.92	0.9992
	σ=624.28						
Log-Normal	μ=0.5751						
	σ=0.032	0.0002	0.475	0.174	0.1047	0.92	0.9999
Log-Pearson Type-III	Cs=0, hence log -Pearson Type III reduces to Log normal distribution Cs(Coefficient of skewness)=N∑(Z-Zbar)^3/(N-1)(N-2)σz^3						

Table 6 shows that as the return period increases, the estimated annual discharge for the Jhelum River at the Sangam gauging station also rises across different distributions. For example, at a 50-year return period, the Normal distribution estimates an annual discharge of 2,034.23 cms, the Log-Normal distribution (LN2) suggests 2,733.11 cms, and the Gumbel distribution predicts 2,390.70 cms. The Log-Normal distribution consistently provides the highest discharge estimates, highlighting how different models can significantly influence flood risk assessments.

Table 6: Flood Frequency estimates of Jhelum River for Sangam gauging station

Return Period (Years)	Pi (Exceedance Probability)	Qi(Non-Exceedance Probability)	w	KT	Annual Discharge cms-Normal Distribution	μ+σ* KT	Annual Discharge cmsLog Normal Distribution(LN2)	Annual Discharge cms Gumbel Distribution
5	0.20	0.80	1.7941	0.84146	1277.14	7.077	1184.72	1209.50
10	0.10	0.90	2.1460	1.28173	1552.00	7.381	1604.77	1578.53
15	0.07	0.93	2.3273	1.50139	1689.12	7.532	1867.11	1786.73
20	0.05	0.95	2.4477	1.64521	1778.91	7.631	2061.70	1932.51
25	0.04	0.96	2.5373	1.75108	1845.00	7.704	2217.78	2044.80
30	0.03	0.97	2.6081	1.83432	1896.97	7.762	2348.76	2136.14
35	0.03	0.97	2.6666	1.90264	1939.62	7.809	2462.01	2213.15
40	0.03	0.98	2.7162	1.96039	1975.68	7.849	2562.00	2279.71
45	0.02	0.98	2.7592	2.01031	2006.84	7.883	2651.69	2338.33
50	0.02	0.98	2.7971	2.05419	2034.23	7.913	2733.11	2390.70

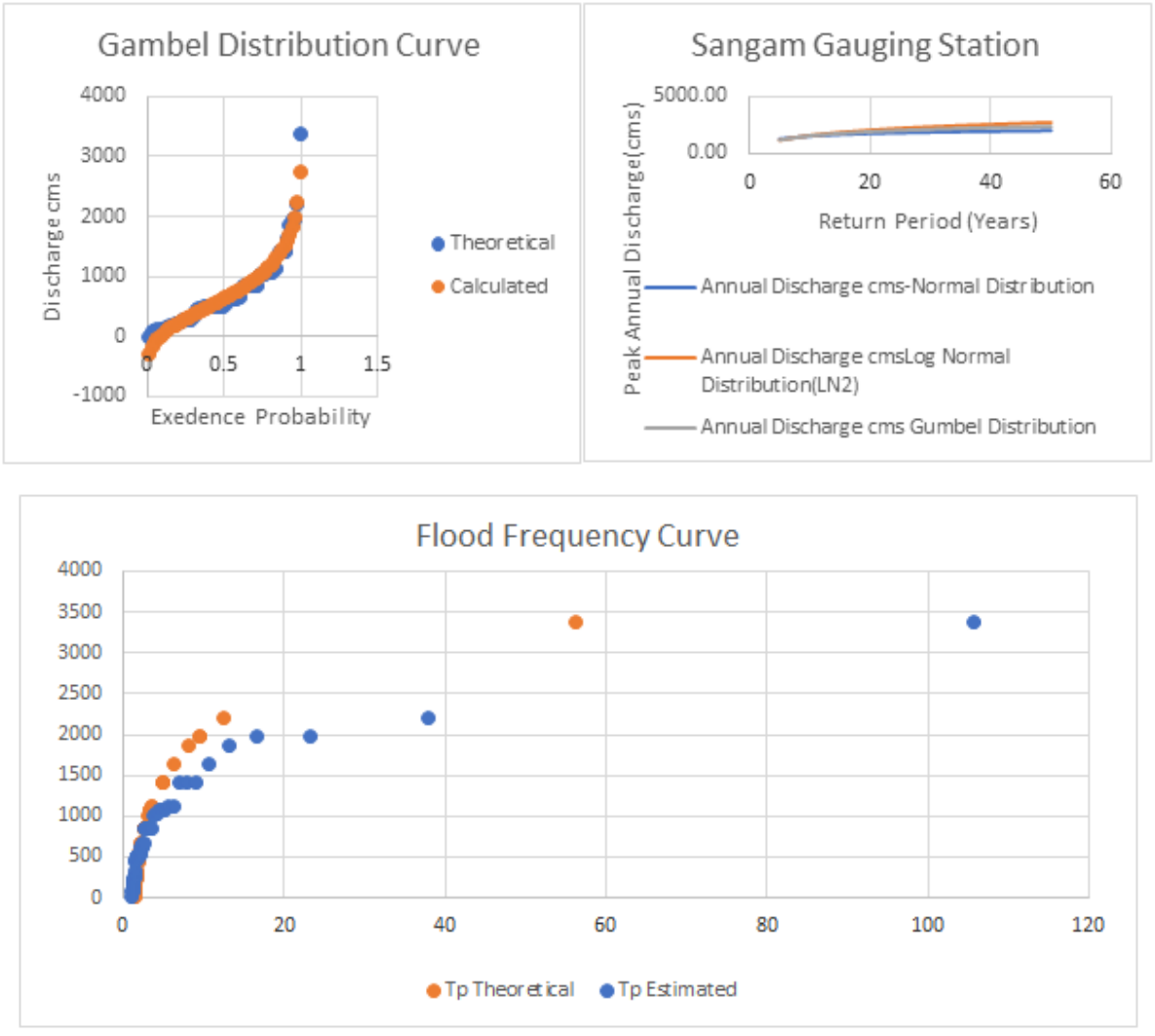

Figure 4: Analysis of Flood Frequency and Discharge Predictions for Sangam Gauging Station

Figure 3 shows a graph of three key elements: The Gumbel Distribution Curve, The Flood Frequency Curve, and the Sangam Gauging Station data. The Gumbel distribution provides a good fit for modeling discharge data, with points generally aligning. The Flood Frequency Curve shows the relationship between return periods and peak annual discharge, with theoretical and estimated values showing an increase with return periods. The Sangam Gauging Station graph compares peak annual discharges calculated using three distribution models (Normal, Log-Normal,

and Gumbel) across various return periods. All three models provide similar estimates of peak discharge, with the Log-Normal distribution estimating slightly higher discharges at longer return periods.

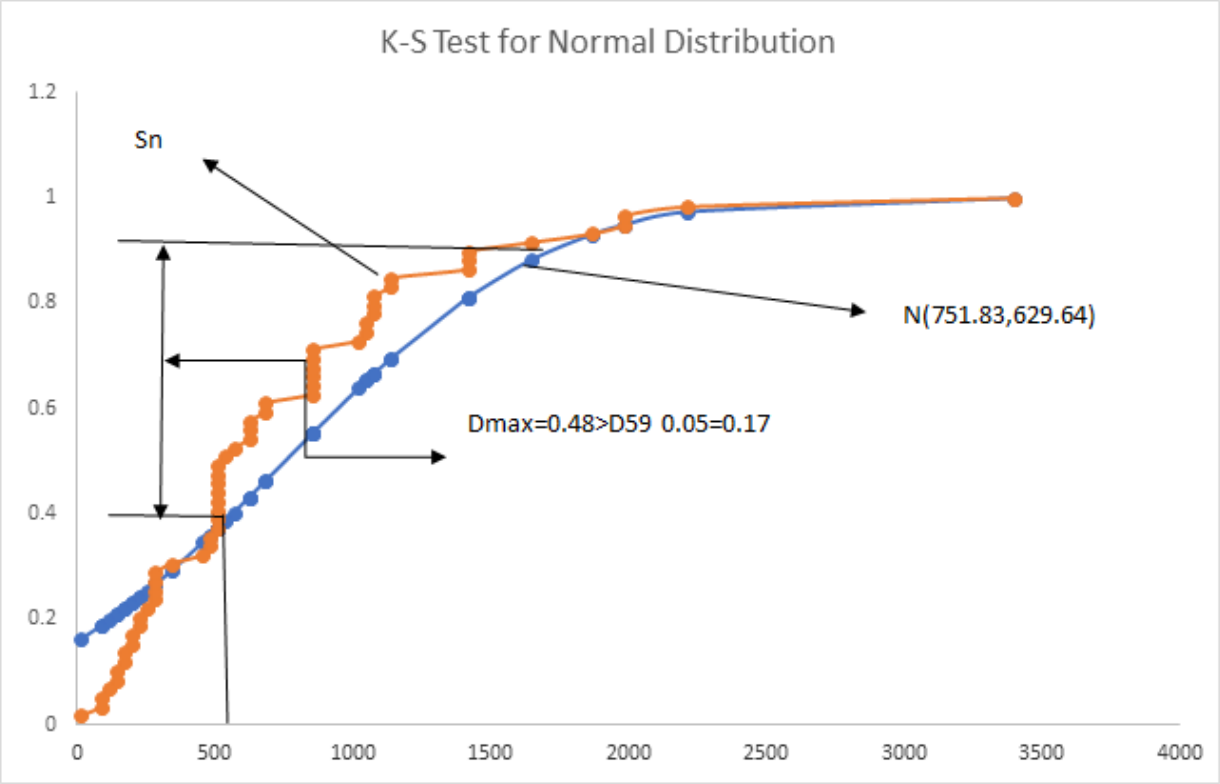

Figure 5: Graph 4 (a): K-S Test

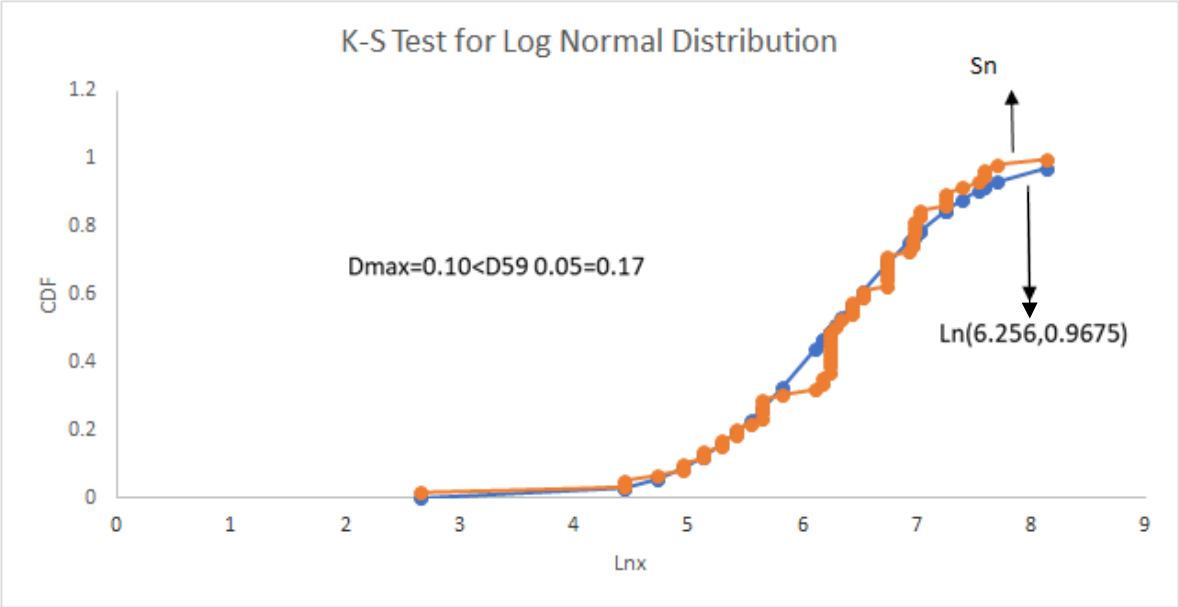

Figure 6: Graph 4 (b): K-S Test

K-S Test also qualifies to Log Normal Distribution as Dmax < Dn^{α}.

3.5 A-D Test for Gumbel Distribution

Table 7: A-D Test for Gumbel Distribution

A^2(A-D Statistic.)	Adjusted. Statistic(A*)	Cα
0.018464	0.0189447	0.757

As Adjusted. Statistic(A*) value (0.0189447) <Critical Value Cα (0.757)

Table 3 and Graph 4 (a) and (b) indicate that only the Log Normal distribution has a qualified chi-square test, and Table 7 shows that the A-D test has a qualified Gumbel Distribution. Also Graph 4 (a) shows a very good fit of distribution for Gumbel distribution. However, it is evident from Table 6 that the calculated peak discharge in 50 years from any distribution cannot supersede the peak discharge of 3398 cm reached in the year 2014. Further, the study considered the goodness of fit by Gumbel distribution and calculated the upper and lower bound peak discharge at a 95% confidence level.

									U_l	L_l
N	y_n	S_n	T_{50}	Y_{50}	K_{50}	x_{50}	b	Se	x_1	x_2
59	0.5527	1.177	50	3.901939	2.845572	2528.276	3.688666	325.6605	3166.570446	1889.981

The upper peak discharge flow during the flood condition 2014 did not cross the 3398cum peak discharge, indicating that a 95% probability of reoccurrence is not possible. Graph 4 (c) shows a Gumbel distribution, allowing for predictions of streamflow values for any return period from 1 to 100 years, with the theoretical distribution represented by orange and the fit of annual peak streamflow data.

Table 8 shows the performance indicators for the Asham gauging station using different statistical distributions. The Normal distribution demonstrated strong performance with an R^2 of 0.94, RMSE of 107.26, and an IA of 0.9999. In contrast, the Log-Normal distribution had a lower R^2 of 0.00 but achieved an RMSE of 0.383 and an IA of 0.9665. The Log-Pearson Type-III distribution, which reduces to Log-Normal due to a zero skewness coefficient (Cs), reflects a similar trend in accuracy.

Table 8: Performance Indicator for Asham gauging station

Distribution		NAE	RMSE	MAE	PA	R^2	IA
Normal	μ=834.62	1.0314	107.2573	0.49566	0.001850237	0.94	0.999886758
	σ=387.88						
Log-Normal	μ=0.7560	0.0002	0.383007	0.19834	0.00	0.78	0.966468497
	σ=0.032						
Log-Pearson Type-III	Cs=0, hence log -Pearson Type III reduces to Log normal distribution Cs(Coefficient of skewness)=N∑(Z-Zbar)^3/(N-1)(N-2)σz^3						

Table 9 shows the flood frequency estimates for the Jhelum River at the Asham gauging station using various statistical distributions. For a 5-year return period, the Normal distribution predicts an annual discharge of 1161.02 cms, the Log-Normal distribution estimates 1178.28 cms, and the Gumbel distribution estimates 1129.93 cms. As the return period increases to 50 years, the predicted discharges rise, with the Normal distribution estimating 1631.42 cms, Log-Normal 1874.07 cms, and Gumbel 1857.45 cms.

Table 9: Flood Frequency estimates of Jhelum River for Asham gauging station

Return Period (Years)	Pi (Exceedance Probability)	Qi(Non-Exceedance Probability)	w	KT	Annual Discharge cms-Normal Distribution	μ+σ* KT	Annual Discharge cmsLog Normal Distribution (LN2)	Annual Discharge cms Gumbel Distribution
5	0.2	0.8	1.794123	0.841456717	1161.018269	7.071812	1178.28133	1129.925021
10	0.1	0.9	2.145966	1.281728757	1331.794635	7.240283	1394.488862	1357.218228
15	0.066666667	0.933333	2.327252	1.501385189	1416.996791	7.324335	1516.765275	1485.455135
20	0.05	0.95	2.447747	1.64521144	1472.785309	7.379371	1602.580896	1575.243329
25	0.04	0.96	2.537272	1.751076531	1513.849138	7.41988	1668.833534	1644.403798
30	0.033333333	0.966667	2.60814	1.834324864	1546.14019	7.451735	1722.850278	1700.667791
35	0.028571429	0.971429	2.666589	1.902639271	1572.638549	7.477876	1768.480523	1748.098015
40	0.025	0.975	2.716203	1.960394917	1595.041287	7.499976	1807.9996	1789.095913
45	0.022222222	0.977778	2.759225	2.01031103	1614.403163	7.519077	1842.865232	1825.199762
50	0.02	0.98	2.79715	2.054188589	1631.422754	7.535867	1874.067863	1857.454459

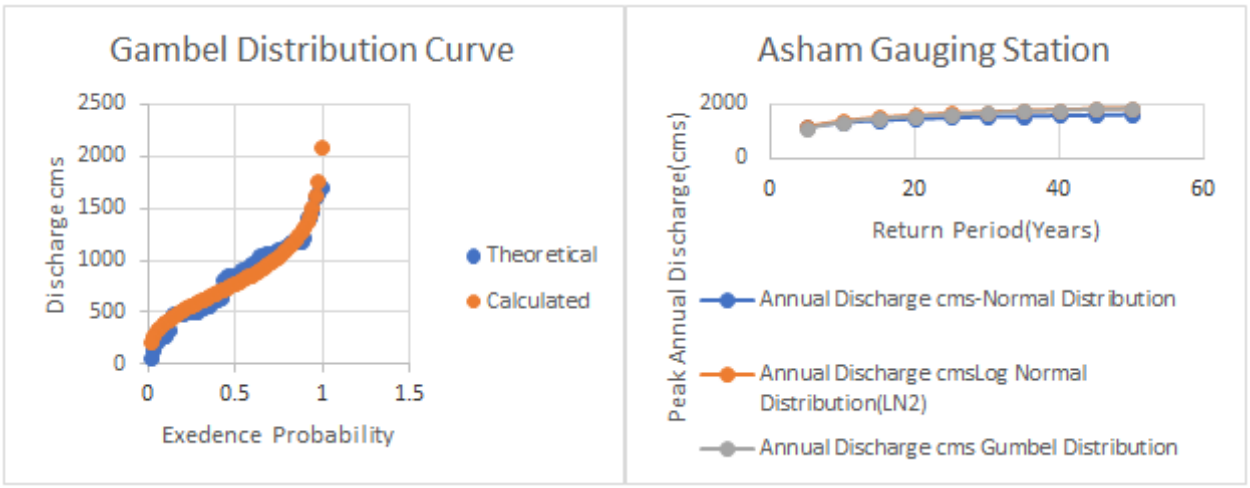

a)

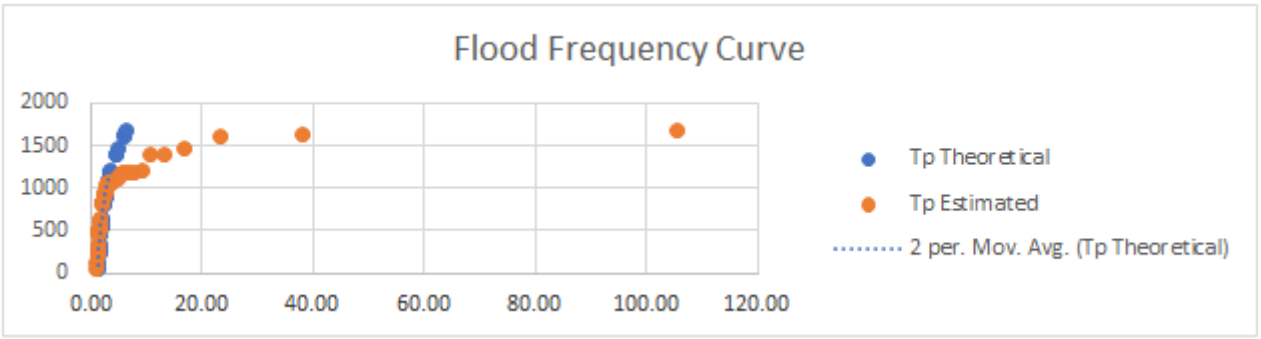

b)

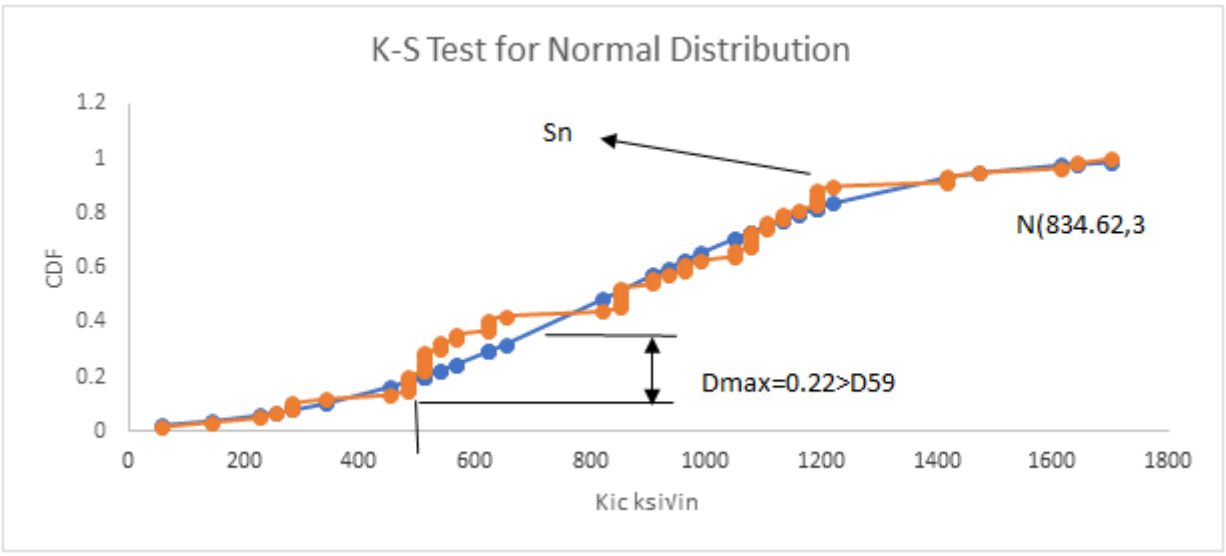

c)

Figure 7: K-S Test

Figure 6 shows The Gumbel Distribution Curve and Flood Frequency Curve, which are used to analyze flood frequency at the Asham gauging station. The Gumbel distribution aligns well with observed data, suggesting similar discharge predictions among the three distributions. The Flood Frequency Curve compares theoretical and estimated peak discharge values over 120 years, indicating the reliability of the estimations. The K-S Test for Normal Distribution evaluates the goodness of fit for the Normal distribution, with closer alignment showing better fit. Overall, the Gumbel and Normal distributions align closely with observed data, validating their use in flood frequency analysis.

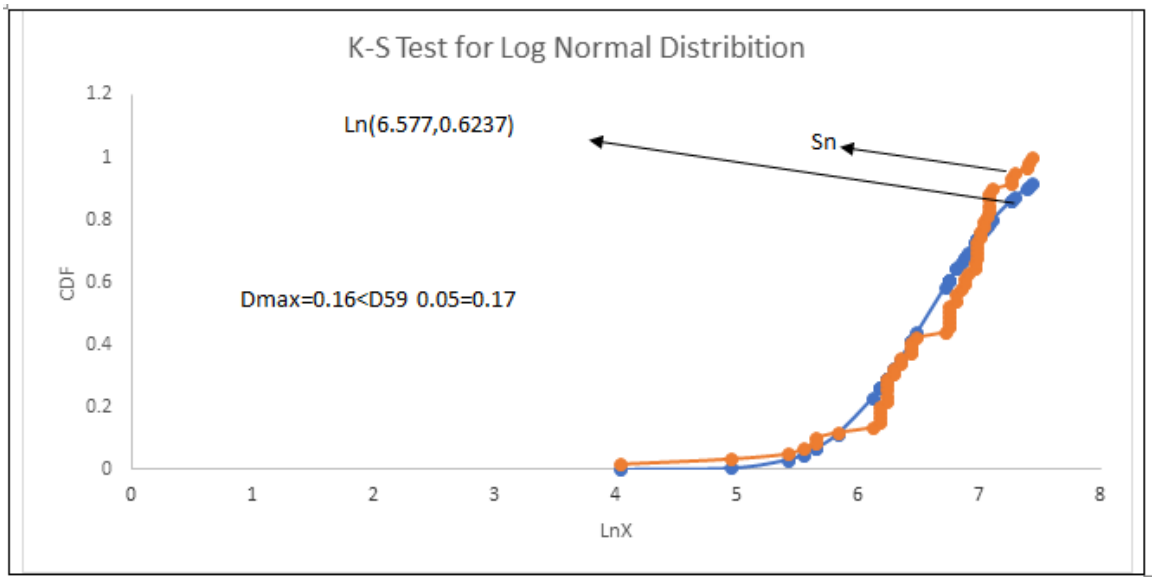

Figure 8: K-S Test for Log Normal Distribution

Figure 7 shows the Kolmogorov-Smirnov (K-S) test, which assesses the fit of a Log-Normal distribution with observed data. It compares the cumulative distribution function (CDF) with the theoretical log-normal distribution, indicating its closeness. The maximum deviation (Dmax) between the two is 0.16, less than the critical value of 0.17. The Log-Normal distribution, with parameters Ln (6.577,0.6237), is considered a good fit for the data, as the Dmax is less than the critical value.

3.6 A-D Test for Gumbel Distribution:

Table 10 shows that the Adjusted Statistic (A* = 0.0189447) for the Anderson-Darling (A-D) test of the Gumbel distribution is significantly lower than the critical value (Cα = 0.757). This indicates that the Gumbel distribution is a good fit for the data, as the A* value is well below the threshold.

Table 10: A-D Test for Gumbel Distribution

A^2(A-D Statistic.)	Adjusted. Statistic(A*)	Cα
0.01846397	0.01894473	0.757

As Adjusted. Statistic(A*) value (0.0189447) <Critical Value Cα (0.757)

									U_l	L_l
N	yn	Sn	T_{50}	Y_{50}	K_{50}	x_{50}	b	Se	x_1	x_2
59	0.5527	1.177	50	3.901939	2.845572	1938.391243	3.688666	202.344289	2334.98605	1541.796

Here, it is observed that the upper peak discharge flow at 95% confidence level crosses the peak discharge of 1699 cum that occurred during the flood condition of the year 2014. Therefore, the probability of reoccurrence at 95% (α = 0.05) is quite possible.

In addition, in graph 6 (c), the line in orange shows the theoretical distribution and the blue line depicts the fit of annual peak stream flow data with the Gumbel distribution. With the help of this curve, one can determine the streamflow values corresponding to any return period starting from 1 year up to 100 years.

Floods are one of the most frequent natural disasters that can impact people and their ability to earn a living. Therefore, flood hazard mapping and flood shelter suitability analysis are important factors in managing land use in flood-prone areas. Application of Remote Sensing (RS) and Geographical Information Systems (GIS) in identifying flood hazard zones and flood shelters are, therefore, important tools for planners and decision-makers (Uddin et al., 2013; Maltare et al., 2023).

A weighted multi-criteria evaluation for mapping flood-prone areas utilizing the GIS wherein criteria with greater impact weights consist of the slope, aspect, soil type, rainfall intensity, flow accumulation, LULC, NDVI, distance from the river, and distance from road announced to find out the impact weight of the nine chosen flood conditioning factors (Alaghmand et al., 2010).

The study also aimed to analyze the Kashmir flood 2014 based on a GIS study to understand better. Accordingly, GIS study has been carried out from different perspectives to undermine the important insights.

As the altitude of Srinagar is 1585m from sea level, an attempt was made to assess the flooded area at different altitudes. The Digital Elevation Model was constructed in ArcGIS 10.8.2 using the USGS database for this exercise, as seen in Figure 8. Selecting SRTM – SRTM 1 Arc-Second Global, data was downloaded. A shape file was created using DIVA.GIS. The lower and upper values of DEM were 1573 and 5531m, respectively.

Using the raster calculator in ArcGIS 10.8.2, rasters were created for 1600 and 1800 m and then converted to polygons to calculate the affected area using the geo area calculator. The study area was 9312 $Km^{2,}$ and the flood-affected area for an altitude of 1600 m was 242 $Km^{2,}$ around 2.59% of the study area. The flood-affected area for an altitude of 1800 m was 1417 Km2, around 15.21% of the study area. This is depicted in Figure 2, which shows that adjacent areas of Srinagar like Pulwama, Awantipora, Anantnag, Chadoora, Badgam, Shopian, Rajpora, Khan Sahib, Beerwah, etc. will be affected if flood covers an area of 1417 Km^2. The entire Srinagar, including the outskirt area, will be affected when flood covers an area of 242 Km^2.

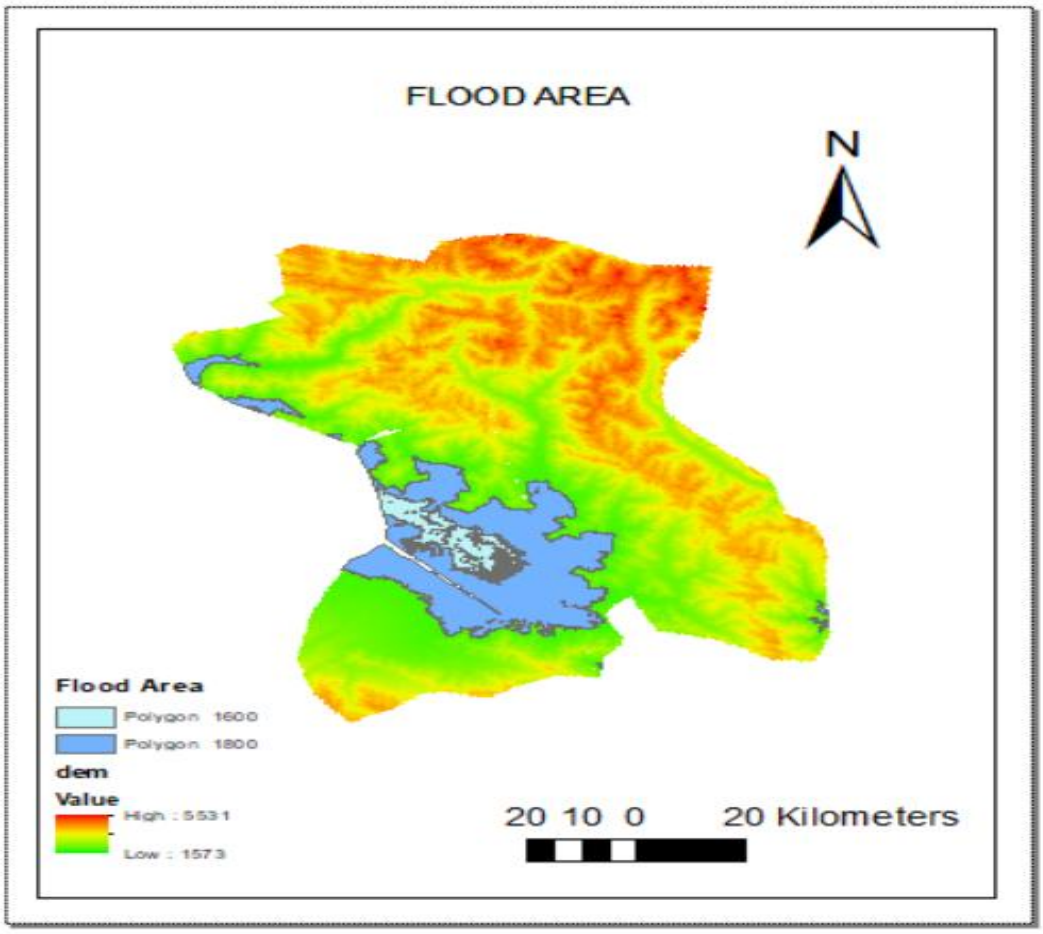

Figure 9: Digital Elevation Model constructed in ArcGIS 10.8.2 and Arc Scene with DEM value (Lower:303 and Upper:6002

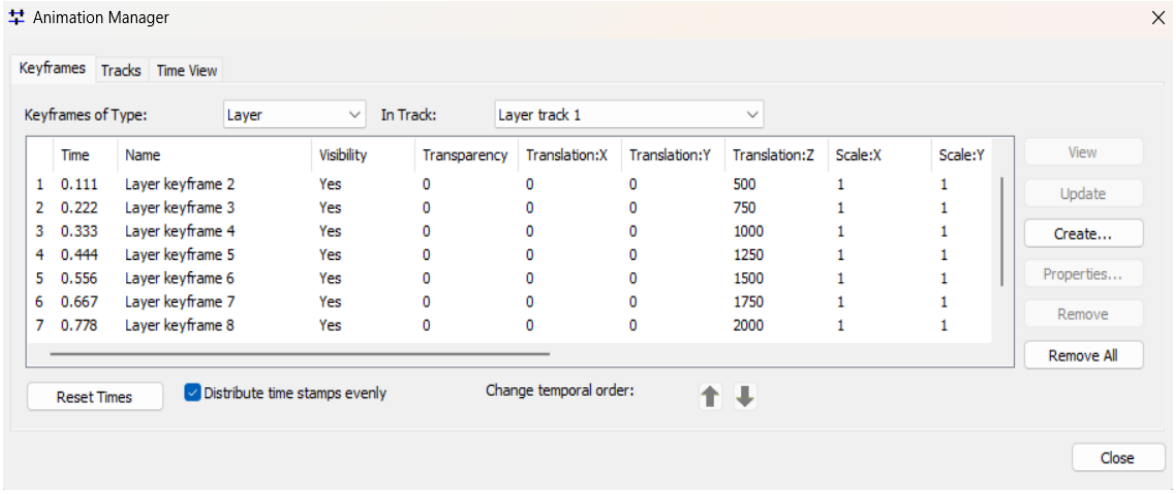

Figure 10: Animation Manager

Figure 9 shows the Animation Manager, which demonstrates a time 0.667 with Z coordinate 1750, i.e., altitude from base height. Fig 4 shows that at time 0.667, the entire valley and its adjacent areas have submerged. This fact also corroborates the findings drawn from Figure 2.

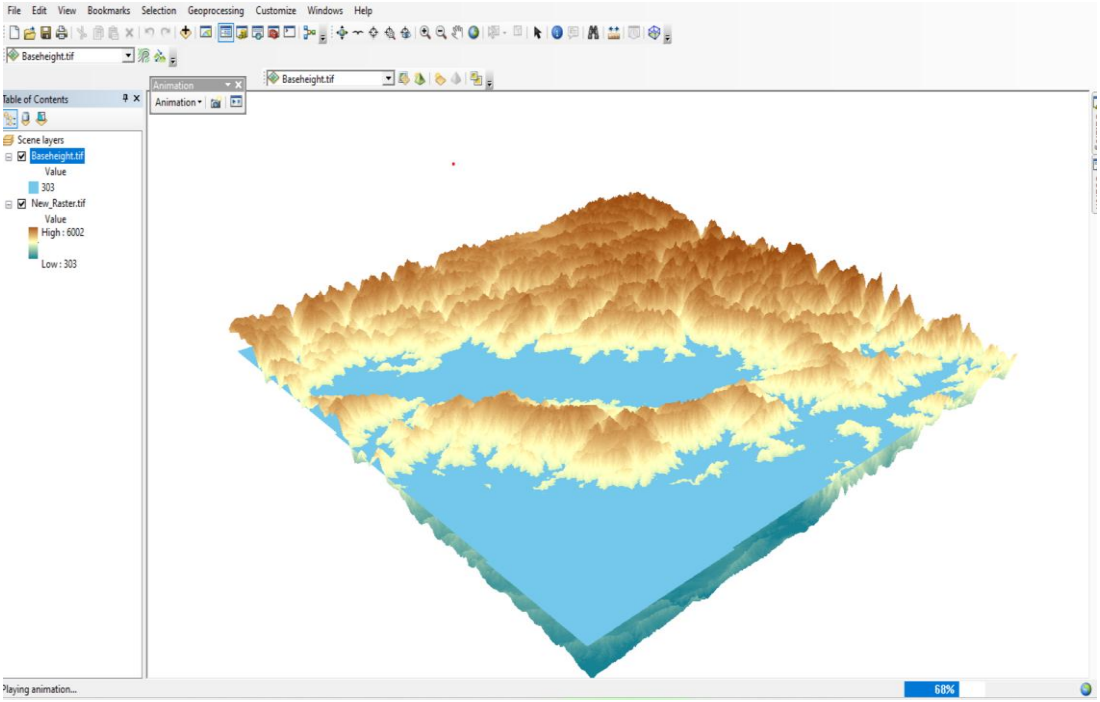

Figure 11: Water shade Delineation model

Further, the Water shade Delineation model was constructed with DEM value (Lower:303 and Upper:6002) and shape file (Lower:1589 and Upper:3912), as seen in Figure 10. Creating rasters of fill, flow direction, flow accumulation, Stream, outlet, and catchment area, eventually, water shade was delineated in the study area.

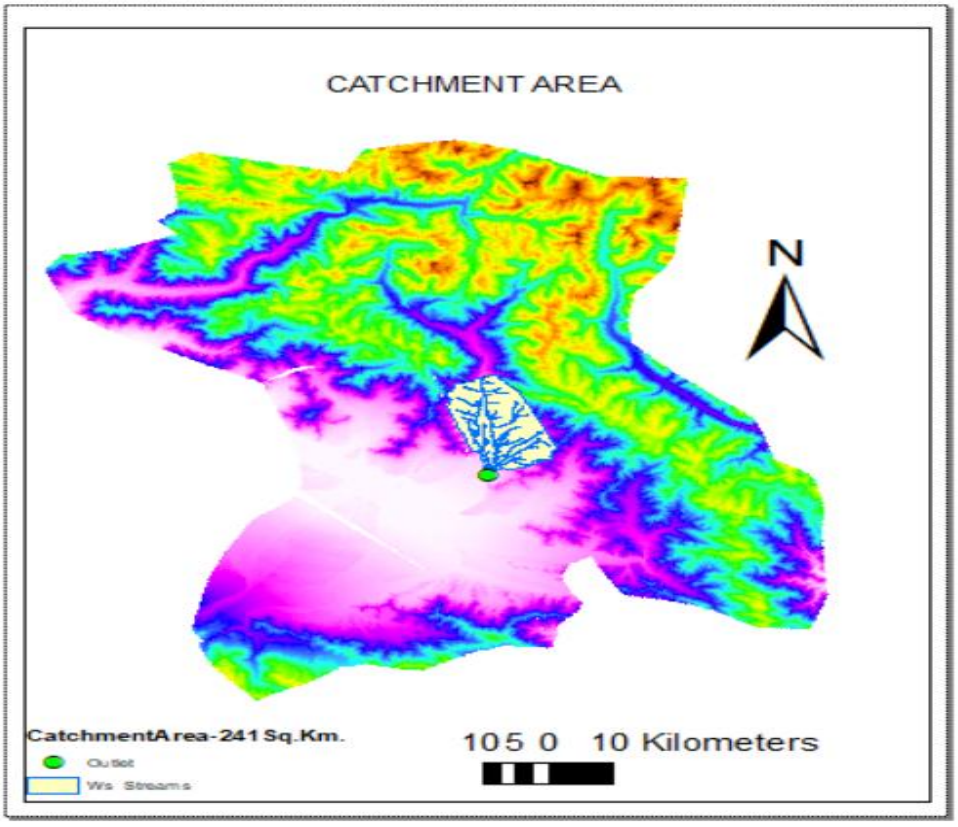

Figure 12: Catchment Area

Figure 11 shows the area of the water shadow stream, also known as the catchment area, which was predicted to be 241 Km² using a geometry calculator and statistics.

Catchments are small tributaries that flow into larger streams or rivers, often found in urban areas or on steep slopes. They influence the biodiversity and ecology of these systems by affecting light, water temperature, pH, nutrient levels, and substrate (Hamid et al., 2020). These characteristics vary naturally as water travels from upper to lower catchments, but human factors such as land use and water flow changes can have a greater impact. A topographic map of a hilly or mountainous area can show where streams begin and join up to create larger sub-catchments.

In this study, flow discharge is being calculated by Rational Method, which is as below:

If R is the total amount of rain in centimeters for a period of T hours, then the mean intensity of rainfall, or I in centimeters per hour, over the storm's whole duration is given by:

$I = \frac{R}{T}$ (3.6) (1)

At a small time interval t, the intensity of rainfall I may be more, as is clear from Figure 12 because the mean value of intensity for the total period T.

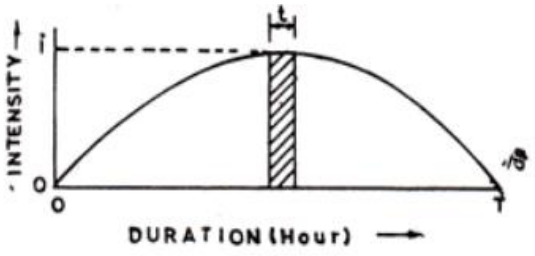

Figure 13: Duration intensity of rainfall

The relation between i and I may be shown as:

$\frac{i}{T} = (T + \frac{C}{t} + C)$

(2)

C is a constant and may be considered unity for all practical purposes.

$i = I\ (T + \frac{1}{t} + 1)$ (3)

If t = one hour and corresponding i is taken as io and the value of I is taken from the above equation

Then,

$$i0 = I\left(T + \frac{1}{2}\right) = \frac{R}{T}(T + \frac{1}{2})$$

$Ic = io\ (\frac{2}{Tc+1})$ (4)

From equation 4, io (One-hour rainfall) can be worked out if the total rainfall R and duration of the severest storm are known. It is advisable to consider several heavy storms spread over a prolonged period. io may be calculated for each case, and the maximum value of U shall be taken as the region's one-hour rainfall for the flood discharge estimation.

From a record of the Meteorological Department, Govt. of India, the values of io for various places of the Indian Union are reproduced in Figure 13.

TABLE 3.2 ONE HOUR RAINFALL, I_o (mm) FOR VARIOUS PLACES *(Khanna)*[6]

Sl. No.	Place	i_o (mm)	Sl. No.	Place	I_o (mm)
1	Agartala	66	2	Ahmedabad	80
3	Aligarh	51	4	Allahabad	65
5	Amin Devi	53	6	Amritsar	74
7	Anantpur	38	8	Asansol	86
9	Aurangabad	61	10	Bagdogra	70
11	Bangalore (Aerodrome)	58	12	Bangalore (Central)	61
13	Barakachar	51	14	Barahkshetra	89
15	Barhi	56	16	Baroda	71
17	Barrackpore	58	18	Bhimkund	00
19	Bhopal	72	20	Bhubaneswar	46
21	Bhuj	49	22	Bishungarh	60
23	Bokaro	58	24	Bombay (Kolaba)	129
25	Bombay (Santa Cruz)	91	26	Calcutta (Alipore)	62
27	Chambal	84	28	Cherapunji	127
29	Coimbatore	80	30	Dhanbad	74
31	Dholpur	47	32	Dibrugarh (Mohanbari)	93
33	Dum Dum	68	34	Durgapur	90
35	Gangtak	81	36	Gauhati	61
37	Gaya	70	38	Gwalior	63
39	Hazaribag	78	40	Hirakud	82
41	Hyderabad	102	42	Imphal	48
43	Indore	60	44	Jabalpur	77
45	Jagdalpur	73	46	Jaipur	55
47	Jamshedpur	62	48	Jawai Dam	98
49	Jharsuguda	77	50	Jadhpur	60
51	Tonk Dam	46	52	Kathmandu	44
53	Kodaikanal	83	54	Konar	59
55	Lucknow	70	56	Madras (Meenambakkam)	62
57	Madras (Nungambakkam)	75	58	Mahabaleswar	51
59	Maithon	54	60	Mangalore	72
61	Marmagao	60	62	Minicoy	70
63	Nagpur	78	64	New Delhi	79
65	North Lakhimpur	65	66	Okha	76
67	Okhaldanga	52	68	Palgauj	56
69	Panaji	54	70	Panambur	37
71	Panchat Hill	71	72	Pathankot	68
73	Patna	59	74	Pokhara	62
75	Pune	47	76	Port Blair	61
77	Punasa	75	78	Raipur	49
79	Ramgarh	56	80	Sagar Island	94
81	Shillong	43	82	Sindri	50
83	Sonepur	78	84	Srinagar	22
85	Shanti Niketan	49	86	Tezpur	63
87	Tiliava Dam	80	88	Tiruchirapalli	78
89	Trivandrum	96	90	Visakhapatnam	63

Figure 14: Values of io for Various Locations in the Indian Union as Recorded by the Meteorological Department, Govt. of India

Sl.No.	Characteristics of the catchment	Value of P
1	Steep bare rock and city pavements	0.90
2	Steep but wooded rock	0.80
3	Plateau lightly covered	0.70
4	Clayey soils, stiff and bare	0.60
5	Clayey soils lightly covered	0.50
6	Loam lightly cultivated and covered	0.40
7	Loam largely cultivated	0.30
8	Sandy soil, light growth	0.20
9	Sandy soil, heavy brush	0.10

Figure 15: Characteristics of the Catchment - Value of P

Sl. No.	Area of catchment in hectares	Value of f
1	Nil	1.0
2	4,000	0.85
3	8,000	0.76
4	12,000	0.70
5	16,000	0.67
6	20,000	0.65
7	40,000	0.62
8	80,000 and above	0.60
N.B. The values of f for intermediate areas may be interpolated		

Figure 16: Area of Catchment in Hectares - Value of f

Time of concentration is defined as the time the run-off takes to reach the bridge site from the furthest point of the catchment, termed the critical moment.

Since the time of concentration is dependent upon the length, slope, and roughness of the catchment, a relationship is established with these factors as below:

$$Tc = \left[\frac{0.89L^3}{H}\right]^{0.385} \qquad (5)$$

Where Tc = Concentration time in hours.

H = Fall in level from the critical point to the site of the bridge in meters.

L = Distance from the critical point to the site of the bridge in Km.

The values of H and L can be found in the contour map of the catchment area.

The critical intensity of rainfall, Ic, corresponding to the concentration-time, Tc, is derived from equation 3.9, considering I = Ic corresponding to T = Tc.

3.7 Estimation of Run-off:

Every centimeter of rainfall over one hectare will produce 100 cu of run-off. m per hour. Hence, a rainfall of Ic cm per hour over an area of A hectare will result in a run-off of 100 A Ic cu. m per hour. If losses due to absorption, etc., are considered, then the run-off is given by:

Q = 100 PI_CA cu. m per hour

$$Q = 0.028\, PI_cA\ cu.m/sec \qquad (6)$$

Where P = Coefficient, which varies according to the porosity of the soil, growth of vegetation, state of initial saturation of the soil, etc.

The values of P for various conditions of the catchment area arc are given in Table 3.3:

3.8 Estimation of Run-off:

One centimeter of rainfall over one hectare gives a run-off of 100 C. m per hour. Hence, Ic cm of rainfall for each hour over A hectares will lead to 100 A Ic cubic cm. m run-off per hour.

If losses due to absorption, etc., are considered, then the run-off is given by:

Q = 100 PI_CA cu.m per hour (7)

$Q = 0.028\ PI_cA\ cu.m/sec$

Where P = Coefficient that is affected by the porosity of the soil and vegetation cover or the initial state of saturation of the soil, etc.

The values of P for various conditions of the catchment area arc are given in Table.

In addition to the coefficient, P, another coefficient, f, is introduced in the run-off formula. As the catchment area gets larger and larger, the possibility of reaching the run-off to the bridge site simultaneously from all parts of the catchment is less and less. As such, the value of f is gradually reduced as the catchment area increases.

$Q = 0.028\ PfIc\ A\ cu.m/sec$ (8)

In the present study, the data are as below:

Catchment Area = 241 Km^2, L=30 km

P = 0.9 from the above-given table

f = 0.62 from the above-given table

R = 120 mm (av.) rainfall during 4-6 Sept. 2014 in Srinagar region (Data from Website)

T = 1 Hr

From Equation 4

io =12/1(1+1/2) =12 cm/hr

From Equation 5

Tc = $[0.89*(30)^3/2323]^{0.385}$ = 1.6

From Equation 4

Ic =12[2/1. +1.6] =9.23cm/hr

From Equation 7

Q = 0.028x0.90x0.62x9.23x24100 = 3470cms

However, as per Govt. data at three gauging stations, i.e., Asham, Sangam and Ram Munshi Bagh

The max. discharge recorded at Sangam Gauging station is 3398cms

Calculated discharge is closer to recorded data by Govt.

3.9 Peak Discharge During Normal Rainy Season:

Now, we calculate peak discharge during normal rainy season:

Catchment Area = 241 Km^2

P=0.9 from the above-given table

f =0.62 from the above-given table

R=70 mm(av.) rainfall during normal rainy season in Srinagar region (Data from Website)

T=1 Hr

From Equation 4

io =7.0/1(1+1/2) =7.0 cm/hr

From Equation 5

$Tc = [0.89*(30)^3/2323]^{0.385} = 1.6$

From Equation 4

Ic = 7.0 [2/1. +1.6] =5.38 cm/hr

From Equation 7

Q = 0.028x0.90x0.62x5.38x24100 = 2024cms

From the above calculation, it is very clear that the existing drainage system of Srinagar and its adjacent areas cannot sustain a peak discharge of more than 2000 cm.

Lastly, flood risk hazard mapping has been carried out in ArcGIS 10.8.2. In developing the flood risk hazard model, the following components have been considered, which play an important role in identifying risk areas.

Elevation (DEM)	-	10%
Slope	-	15%
Land Use/Land Cover	-	10%
Precipitation	-	35%
Proximity to streams/channels	-	30%

The above considerations have been used in developing the model.

Shape file has been created from DIVA.GIS, DEM from SRTM – SRTM 1 Arc-Second Global(USGS), Land Use/Land Cover (2022) from NASA LPDAAC Collections-MODIS MCD 12C1V6.1(USGS) and precipitation data from World Clim- spatial resolutions, between 30 seconds (~1 km2) to 10 minutes (~340 km2)

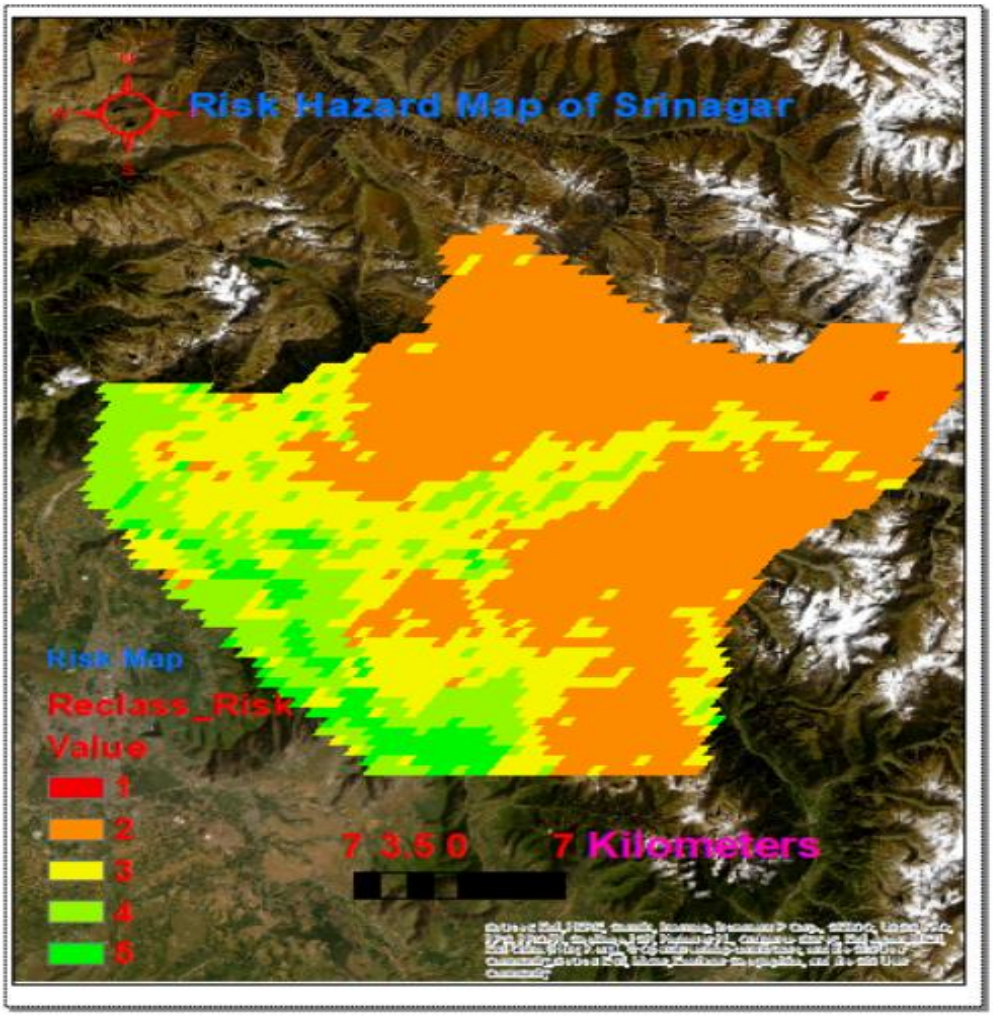

Figure 17: Risk Hazard Map of Srinagar

Figure 16 shows the Risk Hazard Map concept, which labels the risk categories from 1 to 5, with 1 denoting the least risky place and 5 the most dangerous. Accordingly, the north of Srinagar areas, i.e. Kangan, Wangat, Haramukh, Manigam, and Ganderbal, are in the least risk zone. Areas in East and East-South i.e., Kullan, Sonmarg, Baltal, Pahalgam, are in least and moderate risk zone. Area in the west and west-south of Srinagar i.e.Awantipora, Anantnag, Kulgam, Shopian, Pulwama, Kulgam, verinag, Banihal are highly risk zones. These are the areas which were highly affected during the 2014 flood.

CONCLUSION

The Ram Munsi Bagh and Asham Gauging Stations have reported that the peak discharge flow during the 2014 flood did not exceed the threshold value. Still, the upper limit exceeded it within 50 years, indicating the need for safety measures. The Sangam Gauging Station also reported that the peak discharge flow did not exceed the threshold value, indicating the likelihood of a massive flood recurrence in 2014. However, the analysis suggests that suitable mitigation measures should be implemented to prevent chaos and minimize damage. The J&K Govt must formulate a proper framework and policy guidelines to address the devastating economic loss of 20 B$ in direct and 16.74 B$ in indirect losses from the floods. GIS-based models suggest that an altitude of 1600 m, close to the catchment area, covers the flooded area of 242 Km2, indicating the need for increased caution. Flood Risk Hazard Mapping identifies high-risk zones, and the government should focus on improving the outlet/drainage system in Srinagar and its surrounding areas, increasing catchment areas, and enhancing biodiversity and ecology of stream and river systems.

REFERENCE

[1] Aboraya, M., Ali, M. M., Yousof, H. M., & Ibrahim, M. (2022). A novel Lomax extension with statistical properties, copulas, different estimation methods and applications. *Bulletin of the Malaysian Mathematical Sciences Society*, *45*(Suppl 1), 85-120.

[2] Alaghmand, S., bin Abdullah, R., Abustan, I., & Vosoogh, B. (2010). GIS-based river flood hazard mapping in urban area (a case study in Kayu Ara River Basin, Malaysia). *International Journal of Engineering and Technology*, *2*(6), 488-500.

[3] Bera, A. K., Galvao, A. F., Wang, L., & Xiao, Z. (2016). A new characterization of the normal distribution and test for normality. *Econometric Theory*, *32*(5), 1216-1252.

[4] Bhat, M. S., Alam, A., Ahmad, B., Kotlia, B. S., Farooq, H., Taloor, A. K., & Ahmad, S. (2019). Flood frequency analysis of river Jhelum in Kashmir basin. *Quaternary International*, *507*, 288-294.

[5] Collins, L. M., Fidler, P. L., Wugalter, S. E., & Long, J. D. (1993). Goodness-of-fit testing for latent class models. *Multivariate Behavioral Research*, *28*(3), 375-389.

[6] Cox, C., Reeder, J. E., Robinson, R. D., Suppes, S. B., & Wheeless, L. L. (1988). Comparison of frequency distributions in flow cytometry. *Cytometry: The Journal of the International Society for Analytical Cytology*, *9*(4), 291-298.

[7] Crow, E. L., & Shimizu, K. (1987). *Lognormal distributions*. Marcel Dekker New York.

[8] Deshpande, R. (2022). Disaster management in India: are we fully equipped? *Journal of social and economic development*, *24*(Suppl 1), 242-281.

[9] Fayomi, A., Khan, S., Tahir, M. H., Algarni, A., Jamal, F., & Abu-Shanab, R. (2022). A new extended gumbel distribution: Properties and application. *Plos one*, *17*(5), e0267142.

[10] Frances, F., Salas, J. D., & Boes, D. C. (1994). Flood frequency analysis with systematic and historical or paleoflood data based on the two-parameter general extreme value models. *Water resources research*, *30*(6), 1653-1664.

[11] Gaál, L., Szolgay, J., Kohnová, S., Hlavčová, K., Parajka, J., Viglione, A., Merz, R., & Blöschl, G. (2015). Dependence between flood peaks and volumes: a case study on climate and hydrological controls. *Hydrological Sciences Journal*, *60*(6), 968-984.

[12] Gómez, Y. M., Bolfarine, H., & Gómez, H. W. (2019). Gumbel distribution with heavy tails and applications to environmental data. *Mathematics and Computers in Simulation*, *157*, 115-129.

[13] Hamid, A., Bhat, S. U., & Jehangir, A. (2020). Local determinants influencing stream water quality. *Applied Water Science*, *10*(1), 1-16.

[14] Kim, S.-H., & Whitt, W. (2015). The power of alternative Kolmogorov-Smirnov tests based on transformations of the data. *ACM Transactions on Modeling and Computer Simulation (TOMACS)*, *25*(4), 1-22.

[15] Kjeldsen, T., Macdonald, N., Lang, M., Mediero, L., Albuquerque, T., Bogdanowicz, E., Brázdil, R., Castellarin, A., David, V., & Fleig, A. (2014). Documentary evidence of past floods in Europe and their utility in flood frequency estimation. *Journal of Hydrology*, *517*, 963-973.

[16] Kumar, M., Sharif, M., & Ahmed, S. (2020). Flood estimation at Hathnikund Barrage, river Yamuna, India using the peak-over-threshold method. *ISH Journal of Hydraulic Engineering*, *26*(3), 291-300.

[17] Langat, P. K., Kumar, L., & Koech, R. (2019). Identification of the most suitable probability distribution models for maximum, minimum, and mean streamflow. *Water*, *11*(4), 734.

[18] Malik, I. H. (2022). Spatial dimension of impact, relief, and rescue of the 2014 flood in Kashmir Valley. *Natural Hazards*, *110*(3), 1911-1929.

[19] Mishra, A. K. (2015). A study on the occurrence of flood events over Jammu and Kashmir during September 2014 using satellite remote sensing. *Natural Hazards*, *78*(2), 1463-1467.

[20] Payrastre, O., Gaume, E., & Andrieu, H. (2011). Usefulness of historical information for flood frequency analyses: Developments based on a case study. *Water resources research*, *47*(8).

[21] Raschke, M. (2020). Alternative modelling and inference methods for claim size distributions. *Annals of Actuarial Science*, *14*(1), 1-19.

[22] Sahoo, B., & Bhaskaran, P. K. (2016). Assessment on historical cyclone tracks in the Bay of Bengal, east coast of India. *International Journal of Climatology*, *36*(1).

[23] Sahu, P. K., & Sahu, P. K. (2016). Summary Statistics. *Applied Statistics for Agriculture, Veterinary, Fishery, Dairy and Allied Fields*, 35-76.

[24] Sartor, J., Zimmer, K., & Busch, N. (2010). Historical Flooding Events in the German Mosel. *Wasser Abfall*, *12*, 46-51.

[25] Strupczewski, W., Kochanek, K., & Bogdanowicz, E. (2014). Flood frequency analysis supported by the largest historical flood. *Natural Hazards and Earth System Sciences*, *14*(6), 1543-1551.

[26] Uddin, K., Gurung, D. R., Giriraj, A., & Shrestha, B. (2013). Application of remote sensing and GIS for flood hazard management: a case study from Sindh Province, Pakistan. *American Journal of Geographic Information System*, *2*(1), 1-5.

[27] Maltare, N. N., Sharma, D. & Patel, S. (2023). An Exploration and Prediction of Rainfall and Groundwater Level for the District of Banaskantha, Gujrat, India. International Journal of Environmental Sciences, 9(1), 1-17. https://www.theaspd.com/resources/v9-1-1-Nilesh%20N.%20Maltare.pdf

[28] Viglione, A., Merz, R., Salinas, J. L., & Blöschl, G. (2013). Flood frequency hydrology: 3. A Bayesian analysis. *Water resources research*, *49*(2), 675-692.

APPENDIX

TABLE A.5 Critical Values of D_n^+ at Significance Level α in the K-S Test

d.o.f. = n	$\alpha = 0.20$	$\alpha = 0.10$	$\alpha = 0.05$	$\alpha = 0.01$
5	0.45	0.51	0.56	0.67
10	0.32	0.37	0.41	0.49
15	0.27	0.30	0.34	0.40
20	0.23	0.26	0.29	0.36
25	0.21	0.24	0.27	0.32
30	0.19	0.22	0.24	0.29
35	0.18	0.20	0.23	0.27
40	0.17	0.19	0.21	0.25
45	0.16	0.18	0.20	0.24
50	0.15	0.17	0.19	0.23
>50	$1.07/\sqrt{n}$	$1.22/\sqrt{n}$	$1.36/\sqrt{n}$	$1.63/\sqrt{n}$

TABLE A.6 Critical Values of the Anderson-Darling Goodness-of-Fit Test

Table A.6a Critical Values of c_n at Significance Level α of the A-D Test for the Normal Distribution (μ and σ Estimated from Sample Size n)

Significance Level α	a_n	b_0	b_1
0.2	0.5091	−0.756	−0.39
0.1	0.6305	−0.75	−0.8
0.05	0.7514	−0.795	−0.89
0.025	0.8728	−0.881	−0.94
0.01	1.0348	−1.013	−0.93
0.005	1.1578	−1.063	−1.34

Excerpted from D'Agostino and Stephens, 1986 (see References in Chapter 7).

Table A.6b Critical Values of c_n at Significance Level α of the A-D Test for the Exponential Distribution (Parameter λ Estimated from Sample Size n)

Significance Level α	c_n
0.25	0.736
0.20	0.816
0.15	0.916
0.10	0.162
0.05	1.321
0.025	1.591
0.01	1.959
0.005	2.244
0.0025	2.534

Excerpted from Pearson and Hartley, 1972, and D'Agostino and Stephens, 1986 (see References in Chapter 7).

Table A.6c Critical Values of c_a at Significance Level α of the A-D Test for the Gamma Distribution (Parameters Estimated from Sample Data)

	Significance Level α					
k	0.25	0.10	0.05	0.025	0.01	0.005
1	0.486	0.657	0.786	0.917	1.092	1.227
2	0.477	0.643	0.768	0.894	1.062	1.190
3	0.475	0.639	0.762	0.886	1.052	1.178
4	0.473	0.637	0.759	0.883	1.048	1.173
5	0.472	0.635	0.758	0.881	1.045	1.170
6	0.472	0.635	0.757	0.880	1.043	1.168
8	0.471	0.634	0.755	0.878	1.041	1.165
10	0.471	0.633	0.754	0.877	1.040	1.164
12	0.471	0.633	0.754	0.876	1.038	1.162
15	0.470	0.632	0.754	0.876	1.038	1.162
20	0.470	0.632	0.753	0.875	1.037	1.161
∞	0.470	0.631	0.752	0.873	1.035	1.159

Excerpted from Lockhart and Stephens, 1985 (see References in Chapter 7).

Table A.6d Critical Values of c_a at Significance Level α of the A-D Test for the Gumbel and Weibull Distribution (Parameters Estimated from Sample Size n)

Significance Level α	c_a
0.25	0.474
0.10	0.637
0.05	0.757
0.025	0.877
0.01	1.038

Excerpted from Stephens, 1977 (see References in Chapter 7).